A quick and easy way to estimate entropy and mutual information for neuroscience

Mickael Zbili[1], Sylvain Rama[2*]

[1], Lyon Neuroscience Research Center, INSERM U1028-CNRS UMR 5292-Université Claude Bernard Lyon1, Lyon, France.

[2], Laboratory of Synaptic Imaging, Department of Clinical and Experimental Epilepsy, UCL Queen Square Institute of Neurology, University College London, London, United Kingdom.

[*] **Correspondence:**
Sylvain Rama,
s.rama@ucl.ac.uk; rama.sylvain@gmail.com

Keywords: Entropy, Mutual Information, PNG, DEFLATE, Rastergram, Lossless compression, Place Fields

Abstract

Calculations of entropy of a signal or mutual information between two variables are valuable analytical tools in the field of neuroscience. They can be applied to all types of data, capture nonlinear interactions and are model independent. Yet the limited size and number of recordings one can collect in a series of experiments makes their calculation highly prone to sampling bias. Mathematical methods to overcome this so-called "sampling disaster" exist, but require significant expertise, great time and computational costs. As such, there is a need for a simple, unbiased and computationally efficient tool for estimating the level of entropy and mutual information. In this paper, we propose that application of entropy-encoding compression algorithms widely used in text and image compression fulfill these requirements. By simply saving the signal in PNG picture format and measuring the size of the file on the hard drive, we can estimate entropy changes through different conditions. Furthermore, with some simple modifications of the PNG file, we can also estimate the evolution of mutual information between a stimulus and the observed responses through different conditions. We first demonstrate the applicability of this method using white noise signals. Then, while this method can be used in all kind of experimental conditions, we provide examples of its application in patch-clamp recordings, detection of place cells and histological data. Although this method does not give an absolute value of entropy or mutual information, it is mathematically correct, and its simplicity and broad use make it a powerful tool for their estimation through experiments.

1 Introduction

Entropy is the major component of information theory, conceptualized by Shannon in 1948 (Shannon, 1948). It is a dimensionless quantity representing uncertainty about the state of a continuous or discrete system or a collection of data. It is highly versatile as it applies to many

different types of data, it can capture nonlinear interactions, and is model independent (Cover and Thomas, 2006). It has been widely used in the field of neurosciences, see (Borst and Theunissen, 1999; Piasini and Panzeri, 2019; Timme and Lapish, 2018) for a more complete review of work; for example in the field of synaptic transmission (London et al., 2002), information rate of Action Potentials (APs) trains (Bialek et al., 1991; Juusola and de Polavieja, 2003; Street, 2020) or connectivity studies (Ito et al., 2011; Vicente et al., 2011).

However, estimating the entropy of a signal can be a daunting task. The entropy H of a signal X is calculated with the well-known Shannon's formula:

$$H(X) = -\sum_{i=1}^{N} p(x_i) \log_2 p(x_i) \qquad \text{(eq. 1)}$$

Where $p(x_i)$ is the probability that the signal will take the x_i configuration among all the configurations (x_1, x_2, x_3,…, x_N) of the signal. It is considered that if $p(x_i) = 0$, then $p(x_i)\log_2 p(x_i) = 0$, as $\lim_{x\to 0} x\,(\log_2 x) = 0$. And using a base 2 logarithm, entropy will be expressed in bits (Cover and Thomas, 2006; Shannon, 1948).

However, correctly estimating a probability distribution works only if each configuration happens many times. And by definition, one cannot know beforehand the number of needed experiments. This recording bias is even amplified by the fact that without making assumptions, there is no way to determine the relevant quantization and sampling of the data, i.e. in which probability space the entropy must be calculated. The same recordings could be divided in any quantization bins and sampled by any interval, all giving different probability distributions and thus different entropy values.

As an example, let us consider the chain of characters A="04050405". It is unchanged with a quantization range "v" of 5, but will become "01010101" with a quantization range "v" of 2. If we now combine those characters with a bin "T" of 1, this will give a probability distribution of: p(0) = 0.5, p(4) = p(5) = 0.25 in the first scenario (v = 5) and: p(0) = p(1) = 0.5 in the second scenario (v = 2). We thus obtain different entropy values for these two probability spaces: $H^{v=5,T=1} = 1.5$ and $H^{v=2,T=1} = 1$. Now, if we take a combination bin of T = 2 we obtain p(04) = p(05) = 0.5 for v = 5 and p(01) = 1 for v = 2. The calculated entropies thus are: $H^{v=5,T=2} = 1$ and $H^{v=2,T=2} = 0$.

Without making assumptions on the data, there is no way to determine which probability space and which value of entropy is the correct one. Therefore, quantization range and combination bins are crucial to determine the entropy of a signal. In an ideal case, we would need a method able to correct for this sample bias without making assumptions about the signal, and exploring every possible probability space meaning for any length of acquisition, any quantization range "v" and any "T" combination bins of the recorded data.

Thankfully there are multiple ways to use the Shannon's formula (eq. 1) and compensate for this bias, but none of them can be called trivial. There are for example the quadratic extrapolations

method (Juusola and de Polavieja, 2003; de Polavieja et al., 2005; Strong et al., 1998), the Panzeri-Treves Bayesian estimation (Panzeri and Treves, 1996), the Best Universal Bound estimation (Paninski, 2003), the Nemenman-Shafee-Bialek method (Nemenman et al., 2004) or some more recent methods using statistic copulas (Ince et al., 2017; Safaai et al., 2018). Each method has its advantages and downsides (see (Panzeri et al., 2007) for a comparison of some of them), which leaves the experimenter puzzled and in dire need of a mathematician (Borst and Theunissen, 1999; Magri et al., 2009; Piasini and Panzeri, 2019; Timme and Lapish, 2018).

However, there is another way to calculate the entropy of a signal, through what is called the Source Coding Theorem (Cover and Thomas, 2006; Larsson, 1996, 1999; Shannon, 1948; Wiegand, 2010). In signal processing, data compression is the process of encoding information using fewer bits than the original representation. In case of lossless compression, it does so by sorting parts of the signal by their redundancy and replacing them by shorter code words (Huffman, 1952; Shannon, 1948). Interestingly, the Source Coding Theorem specifies that it is impossible to compress a signal of size S such that the length of the compressed signal is smaller than the entropy rate of the original signal multiplied by S. Therefore, with a perfect compression method the size of the compressed signal is proportional to the original signal entropy (Cover and Thomas, 2006; Larsson, 1996, 1999; Shannon, 1948; Wiegand, 2010). This method has been widely described in the field of physics, where estimating entropy via compression algorithms has been done several times (Avinery et al., 2019; Baronchelli et al., 2005; Martiniani et al., 2019, 2020) but to our knowledge it has been used only twice in the field of neurosciences (Amigó et al., 2004; London et al., 2002) to estimate the entropy of spike trains and the information efficacy of a synapse.

When choosing this way of calculating entropy, the choice of the compression algorithm becomes critical as the compressed signal must be the smallest possible in order to represent the entropy of the original signal. It is of course possible to craft its own compression algorithm (see (London et al., 2002)), but thankfully this application has been broadly used in the domain of informatics, in order to compress text and images efficiently on the hard drive of a computer or before sending data through a network. In particular, this led to the development of two principal entropy-coding compression algorithms: the Huffman coding algorithm (Huffman, 1952) and the the Lempel–Ziv–Storer–Szymanski algorithm (Storer and Szymanski, 1982; Ziv and Lempel, 1977), both used to compress text and image files. This Lempel-Ziv algorithm and its variants are the main tools for the estimation of entropy from data compression (Avinery et al., 2019; Baronchelli et al., 2005; Benedetto et al., 2002; Martiniani et al., 2019).

Portable Network Graphics (or PNG, see specifications at https://www.w3.org/TR/PNG/ or http://www.libpng.org/pub/png/) is a graphic file format supporting lossless data compression. Its high versatility and fidelity made it widely used for saving and displaying pictures. Its lossless compression is based on the combination of the Lempel–Ziv–Storer–Szymanski and Huffman algorithms and is called DEFLATE (Deutsch, 1996). Its great efficacy made it a reference for comparison with other entropy-encoding image compression methods (Bian et al., 2019; Cover

and Thomas, 2006; Hou et al., 2020; Mentzer et al., 2020) and it is even used directly to estimate image entropy (Wagstaff and Corsetti, 2010).

In this paper, we show that measurement of PNG file output size of neuroscientific data (in Bytes on the hard drive) is a reliable and unbiased proxy to estimate the level of entropy of electrophysiological or morphological data. First, the relationship between entropy level and file size is linear. Second, by simply dividing the size of the PNG file (in Bytes) by the number of pixels in the image, we can obtain a "PNG Size Rate" (or "PNG Rate", in Bytes per pixels), which slowly converges towards a stable value when increasing the amount of recorded data. This allows the experimenter to compare multiple recordings of different sizes. Therefore, even if the PNG Rate does not provide the exact entropy value, it is robust enough to estimate the level of entropy in response to different experimental conditions. Furthermore, with minimal modifications of the PNG file, we validate estimation of the mutual information between a stimulation protocol and the resulting experimental recording.

2 Materials and Methods

2.1 Neuronal modeling

A single compartment model was simulated with NEURON 7.7 (https://www.neuron.yale.edu/neuron/). All simulations were run with 100-µs time steps. The nominal temperature was 37°C. The voltage dependence of activation and inactivation of Hodgkin-Huxley–based conductance models were taken from (Hu et al., 2009) for g_{Nav} and g_{KDR}. The equilibrium potentials for Na^+, K^+, and passive channels were set to +60, −90 and −77 mV, respectively. The conductances densities were set to 0.04 S/cm^2, 0.01 S/cm^2 and $3.33*10^{-5}$ S/cm^2 for g_{Nav} and g_{KDR} and passive channels, respectively. The model was stimulated using various numbers of excitatory synapses using the AlphaSynapse PointProcess of the NEURON software. The time constant and reversal potential were the same for every synapses and were set to 0.5 ms and 0 mV, respectively. The size of EPSPs produced by the synapses were randomly chosen using a lognormal distribution of EPSPs amplitude experimentally described in L5 pyramidal neurons (Lefort et al., 2009). Each synapse stimulated the model once during a simulation and the time onset was randomly chosen.

For the simulations of Figure 3, the number of synapses simulating the model depended on the duration of the simulation and spiking frequency desired. For example, to calculate the entropy rate in the case of a 1 Hz spiking frequency during 400 seconds, we simulated the model with 3200 of the synapses described above. For higher spiking frequencies, the number of synapses were increased.

For the simulations of Figures 4A and 4B, each trace lasted 5 seconds. The number of synapses simulating the model depended on the spiking frequency desired. For example, to calculate the

information transfer rate in the case of a 1 Hz spike train, we simulated the model with 400 of the synapses described above. We ran 20 trials of the simulation with the same train of synapses (Figure 4A). In order to introduce some jitter in the spiking times, we also injected a small gaussian current with a mean of 0 nA and a standard deviation of 0.0005 nA during the 5 seconds of the simulation. We reproduced this whole protocol for others desired spiking frequency, using increasing number of synapses (for example: 1900 synapses for a 19 Hz spiking).

For the simulations of Figure 4C, we stimulated the model with 750 of the synapses described above to get a spiking frequency around 5Hz. The time onsets and the amplitude of the synapses were randomly chosen at each simulation. We also added one supplementary synapse (Syn_supp) which stimulates the model every 200 ms (i.e 25 times in 5 s). The size of the EPSP size produced by this synapse was called wSyn_supp. When wSyn_supp was weak, this synapse did not drive the spiking of the model (Figure 4C, up left). When wSyn_supp was strong, this synapse drove the spiking of the model (Figure 4C, down left). We ran 100 simulations for each wSyn_supp.

2.2 Direct calculation of entropy rate and mutual information rate via the direct method and quadratic extrapolation

We calculated the entropy and mutual information rates using the direct method and quadratic extrapolation, as originally described by (Strong et al., 1998) and recently used by (Juusola and de Polavieja, 2003; Panzeri et al., 2007; de Polavieja et al., 2005). This method consists in two steps:

i) The first step of this method, comparable to a “brute force” approach, is to calculate the different values of entropy rates of the signal for multiple probability spaces, i.e. with multiple portions “Size” of the signal, multiple quantization ranges “v” of the signal values and multiple combination bins “T” of each value. As described in the introduction, each modification of “Size”, “v” or “T” will give a different value for the entropy. Ideally, we would like to calculate it for every possible values of “Size”, “v” and “T”, but this is not possible in practice: we want an estimation of entropy rate for recordings of infinite size, quantization range and combination bins. We thus limit ourselves to probable combinations for this first step, keeping in mind we will need a set of values big enough to yield accurate fits in the second step.

For example, in figure 1A, to estimate the entropy rate on different length of recordings the parameter “Size” was successively set as 1, 0.9, 0.8, 0.7, 0.6, 0.5, which takes decreasing portions of the signal, from full signal to half of it. As we are measuring the entropy rate from uniform white noise with 2 to 256 possible values, we successively set the quantization range “v” as 2, 4, 8, 16, 32, 64, 128, and 256. Any range higher than 256 will yield the same value of entropy rate. The number of combination bins “T” was successively set as 1, 2, 3, 4, 5, 6, 7, 8, in order to measure the entropy with no combinations (T=1) until 8 possible combinations of values

(T=8). This produced 6 * 8 * 8 = 384 distinct values of entropy for every trial. Entropy values for different trials of the same condition were averaged together.

ii) The second step (Figure 1B) will extrapolate these data to find their limit value to infinite size, quantization range and combination bins. The previously calculated values are first plotted against 1/Size and the intersections to 0 estimated by quadratic fit of the data. This gives us the entropy values for every "v" and "T", corrected for infinite size of the recordings. These values are then quadratic fitted against 1/v. The intersection to 0 gives us entropy values for every number of combination "T", corrected for infinite Size and infinite number of quantization levels "v". As combinations of T elements will happen 1/T times, we divide these values by T and these new values are fitted against 1/T to estimate the extrapolation to 0. By performing this triple extrapolation and dividing by the number of combination bins, we can estimate the entropy rate R_S of the signal for theoretical infinite size of recording, infinite number of quantization levels and infinite number of combinations as

$$Rs = \lim_{T\to\infty} \frac{1}{T} \lim_{v\to\infty} \lim_{Size\to\infty} H^{T,v,Size} \qquad \text{(eq. 2)}$$

To obtain R_N in Figure 4, the entropy rate of the noise, instead of calculating the entropy H along the length of the signal, we did it at every time point across the successive trials. This is equivalent to simply transpose the signal and re-applying the same method than for R_S. Finally, we obtained the mutual information rate by subtracting R_N to R_S as

$$R = R_S - R_N = \lim_{T\to\infty} \frac{1}{T} \lim_{v\to\infty} \lim_{Size\to\infty} \left(H_S^{T,v,Size} - H_N^{T,v,Size}\right) \qquad \text{(eq. 3)}$$

For Figure 4A, simulated recordings were down-sampled to 10 kHz before calculation of information rate. For Figure 4C, middle, simulated recordings were down-sampled to 3 kHz and binned as 0 & 1 depending of the presence of Action Potentials or not, similar to (London et al., 2002).

For figures 1B, 1C, 1D, 2, 3, 4A and 4B, The parameter "Size" was successively set as 1, 0.9, 0.8, 0.7, 0.6, 0.5; "v" successively set as 2, 4, 8, 16, 32, 64, 128, 256 and the parameter "T" was successively set as 1, 2, 3, 4, 5, 6, 7, 8. For figure 4C, the parameter "Size" was successively set as 1, 0.9, 0.8, 0.7, 0.6 and 0.5; "v" set as 2 and the parameter "T" was successively set as 1, 2, 5, 10, 20, 30 and 40. R_S, R_N and information transfer rate were calculated by direct method and successive quadratic extrapolations, as described above.

All of this was done by custom scripts written in Python 3.7 Anaconda with Numpy, Pandas and pyABF modules. These scripts are available at https://github.com/Sylvain-Deposit/PNG-Entropy.

2.3 Export to PNG format

Export to PNG was made with 3 different softwares: i) Anaconda 3.7 (https://www.anaconda.com/) and the pyPNG package (https://pypi.org/project/pypng/) for

Figures 1, 2A, 3A, 3B ; ii) Labview 2017 and Vision 2017 (National Instruments) for Figures 2B, 3C, 4A-C, 5C; iii) the FIJI distribution of ImageJ software (Rueden et al., 2017; Schindelin et al., 2012) for figure 6C. Signals were normalized to 256 values from 0 to 255 simply by subtracting the minimal value of the signal, then dividing by the maximal value and multiplying by 255. It was then saved as PNG format in 8-bits range (256 grey values). For figure 4C, as the signal was binnarized we saved it with a 1-bit range (2 grey values).

A minimal file of PNG format is composed of a header and several parts of data, named critical chunks (https://www.w3.org/TR/PNG/#5DataRep). To these minimum requirements it is possible to add ancillary chunks (https://www.w3.org/TR/PNG/#11Ancillary-chunks) containing various information such as Software name, ICC profile, pixels dimensions, etc… If useful, this is hindering the estimation of entropy as it represents an overhead to the final size of the file. To estimate this overhead for each of our software we saved an image of 100 * 100 values of zeros, which corresponds to black in 8-bits grey levels and has an entropy of 0. With pyPNG, Fiji and Labview we obtained three PNG files of size 90, 90 and 870 Bytes, respectively. When repeating the experiment of figure 1, we obtained really similar linear fits of slopes 1.21 (R^2 = 0.99), 1.18 (R^2 = 0.99) and 1.21 (R^2 = 0.99) respectively.

For Figure 6C, we used Fiji for every image of the collection and we: i) extracted the channel number 2 containing the MAP2 staining; ii) converted the file to 8-bits grey levels; iii) thresholded it to remove every intensity values under 10 to remove most of the background; iv) saved the new file as PNG format, v) checked the size of this new file and vi) divided the size in kBytes by the number of soma visible in the field.

3 Results

3.1 Entropy estimation in uniform white noise signals

To test the usability of the PNG format to represent entropy, we started by generating 10 000 pixels of uniform white noise which could take 2 values (Figure 1A, 2 grey values). As we are using white noise, we fully know the probability distribution (in that case, $p(xi) = 1/N$), we can apply the eq. 1 and obtain an entropy H of 1 bit. We then repeated this noise model progressively increasing the number of possible values by power of 2 until 256 (i.e 4 possible values, 8 possible values, 16 possible values etc… up to 256 possible values). The 256 possible values white noise corresponds to an entropy of 8 bits (Figure 1A). The entropy rate R is defined as $R = \frac{1}{T} H$ with T being the sampling of the signal. In this model case, we can take T = 1 (i.e a sampling of 1 pixel) to finally obtain an entropy rate in bits per pixel.

As a control way to calculate the entropy of our signals, we used a method described in (Juusola and de Polavieja, 2003; Panzeri et al., 2007; de Polavieja et al., 2005; Strong et al., 1998), involving the use of the Shannon's formula in many probability spaces followed by quadratic extrapolations to estimate the entropy rate in a case of an infinite size signal, an infinite

quantization and an infinite time sampling, see Methods for explanations. This method allows the exact calculation of the signal entropy rate but is long to compute and needs programming skills to be implemented. It will be used all along this study as a control to be compared with the PNG method. It will be referred as "the quadratic extrapolations method".

In our simple model data, we can see that when using only 2 different values for the white noise (Figure 1B), the quadratic extrapolations method gives an entropy rate really close to 1 bit/pixels as expected (Figure 1B, right panel, black arrowhead).

However, when increasing the number of white noise possible values until 256 (real entropy rate H of 8 bits/pixels) we start to unravel the so-called "sampling disaster" (Figure 1C). In fact, the quadratic extrapolations method gives a value around 5.7 bits/pixels (Figure 1C, right panel, red arrowhead), far from the expected one. This is easily explained by the number of data points we have in our model signal. The last extrapolation concerns the "T" combinations of values to calculate the entropy rate and when using uniform white noise and with T equal to 1, it means we need at least $2^8 = 256$ points to properly estimate the probability distribution. However, if T increases to 2 (1/T = 0.5 in the Figure 1C), we then need at least $2^{8*2} = 65536$ points to estimate the probability distribution, when we had only 10000. The probability distribution is thus insufficient to properly estimate the entropy rate of this signal with 256 values. Even by using quadratic extrapolations to compensate for the sampling bias, we can see it gives a wrong result for high entropy values when there is not enough data points (red arrowheads in Figure 1D, left panel).

As a comparison, we simply saved the 10 000 pixels data of increasing noise (Figure 1A) as PNG image file with a depth of 8 bits (and thus 256 possible values). We measured the space taken by these files on the hard drive (in Bytes) and divided this value by the number of pixels to obtain the PNG Rate (in Bytes/pixels) (Figure 1D, right panel). The PNG Rate was linearly correlated with the real entropy rate ($y = 0.12\,x + 0.06$, $R^2 = 0.99$). The PNG compression algorithm works with linearized data, which means there is no difference when saving pictures as a 100 * 100 square format (figure 1D, right panel, squares plot) or saving a 10 000 single line (same panel, crosses plot). From this first test, we can conclude that the size of a PNG file of a model signal has a linear relationship with its entropy rate.

To better investigate the effect of recording length on entropy rate and PNG conversion, we generated a signal of 100 points of uniform white noise with 2 possible values (0 and 1) and progressively increased the percentage of 1 in this signal, from 0 to 100% (0 is represented by a black pixel, 1 is represented by a white pixel) (Figure 2A). As we know the ideal probability distribution of this signal, we can use the Shannon's formula (eq.1) to calculate the real entropy rate and obtain the bell-shaped curve as described by (Shannon, 1948) (Figure 2A, middle, black dashed curve). However, we see that if we calculate the entropy rate from our 100 points signal with the quadratic extrapolations method (Figure 2A, middle, light grey), the curve obtained is far from ideal: it is unable to reach the proper value of 1 for maximum entropy. This is another

example of sampling disaster. We have to increase the number of points in our signal up to 10 000 points to obtain a maximum entropy rate corresponding to the maximum ideal entropy rate (Figure 2A, middle, middle grey and dark grey). Then, we saved the same signals to PNG files, measured their size on the hard drive and divided by the number of pixels to obtain the PNG Rates of each signal. Finally, we normalized the obtained curves to compare their shapes (Figure 2A, right). We can see that the obtained curve progressively fits the ideal entropy rate curve when the number of points increases (Figure 2A, right), but at a slower rate than the direct method. In fact, even with 10 000 points, the curve obtained by the PNG method does not fit perfectly the ideal curve.

As an illustration of the effect of the number of points on each method, we generated signals of uniform white noise with increasing number of possible values from 0 to 256 (thus entropy rates from 0 to 8 bits per point) and we increased the number of points in these signals from 1000 to 1000 000 points (Figure 2B). We used the quadratic extrapolations method to calculate the entropy rates, and saved the same signals as PNG files to obtain the PNG rate. When plotted against the ideal entropy rate, we can see that these two methods yield different behaviors (Figure 2B). When calculating the entropy rate by the quadratic extrapolations method, the sampling bias dramatically modifies the high values of entropy rate and we obtain biphasic curves (Figure 2B, left). This indicates that we cannot estimate high entropy values with short signals. However, the values are perfectly accurate for low entropy rates or if the number of points in the signal is sufficient (around 100 000 points in this case). When plotting the PNG rate, we can see that the relationship between PNG Rate and the ideal Entropy Rate is always linear, but the number of points affects the slope and intercept of the obtained curve (Figure 2B, right). This relationship converges towards a stable curve for long signals (around 100 000 pixels). This means that if we have multiple signals of the same size, we can properly estimate the modifications of entropy rate between them as the relationship with entropy rate is linear. However, if we have signals of different sizes, we have to check if the PNG rate converged to a stable value to be able to compare them.

To estimate the number of points needed for a correct entropy rate estimation of a given signal, we generated uniform white noise signals of 100, 500, 1000, 5000, 10 000 and 20 000 points. Those signals could present either 2 possible values (Figure 2C, left) or 4 possible values (Figure 2C, right). First, we calculated their entropy rates by the quadratic extrapolations method and plotted them versus their number of points (Figure 2C, white circles). When using a uniform white noise signal with 2 possible values (ideal entropy rate of 1 bit per point), 500 points were enough to find the optimal value of entropy rate by the quadratic extrapolations method (Figure 2C, left, white arrowhead). If we increase the number of values in our generated signal to 4 possible values (ideal entropy rate of 2 bits per point), the quadratic extrapolations method needs 1000 points to find the optimal value of entropy rate (Figure 2C, right, white arrowhead). Second, we saved all the generated signals to PNG files, measured their size in Bytes on the hard drive and divided these sizes by the number of pixels in the image file to get the PNG Rates of the

signals. Then, we plotted the PNG Rates versus the number of points in the signals (Figure 2C, black squares). When using a uniform white noise signal with 2 possible values (ideal entropy rate of 1 bit per point), we can see that the PNG Rate reaches a stable value around 10 000 pixels (Figure 2C, Left, black arrow). With a uniform white noise with 4 possible values (ideal entropy rate of 2 bits per point), the PNG rate reaches a stable value around 10 000 pixels as well (Figure 2C, Right, black arrow). By this experiment, we concluded that both methods converge towards a stable solution. However, the quadratic extrapolations method is much quicker to converge than the PNG Rate method.

From these examples, we conclude that the number of points in the signal is critical to capture its entropy rate. In the case of short signals, the quadratic extrapolations method gives biphasic relationships with the Entropy Rate, making it unsuitable to calculate high entropy values. The PNG Rate method stays linear to the Entropy Rate, which allows comparing files of the same size in a wide range of entropy values. Both methods converge to a stable solution when increasing the number of points in the signal, but the PNG Rate method convergence is slower. Both methods allow comparing multiple signals of different sizes, as long as the stable value is reached.

3.2 Entropy estimation in electrophysiological signals

In order to test the ability of the PNG Rate method to estimate the entropy of electrophysiological signals, we created a single compartment model in NEURON 7.7. The model contained sodium and potassium voltage-dependent channels to allow the spiking (see Methods for model description). The model was stimulated using various numbers of EPSPs with amplitudes chosen randomly in a log-normal distribution described in (Lefort et al., 2009). Each synapse stimulated the model once during a simulation and its time onset was randomly chosen. By increasing the number of synapses stimulating the model, we could increase the spiking frequency.

We ran 20 trials of 5 seconds with an increasing number of synapses, to obtain model traces ranging from 1 to 20 Hz AP frequency (Figure 3A, left). We used the quadratic extrapolations method to calculate the Entropy Rate on all our model traces. In parallel, we saved these traces as 8-bits PNG files and divided by the number of points in the image to obtain the PNG Rate. As expected, the PNG Rate has a linear behavior versus the Entropy Rate (Figure 3A, right). As a control, we measured the Entropy Rate and the PNG Rate for different sizes of model traces at 1, 10 and 20 Hz, ranging from 1 second to 400 seconds. In our conditions, the Entropy Rate converges to a stable value in around 5 seconds of recordings (or 50 000 points, Figure 3A, top left), whereas the PNG Rate needs around 40 seconds of recording (or 400 000 pixels, Figure 3A, bottom left). These can be considered as the minimal time needed if one wants to compare multiple files of different sizes. Interestingly, as the PNG algorithm works with linearized data, there is no difference between 40 seconds of recordings and 8 sweeps of 5 seconds each. This

means that in our model case, 20 trials of 5 seconds each were largely enough to estimate the stable value of the PNG Rate.

3.3 Mutual Information estimation in electrophysiological data

Most of the time, the experimenter is not interested in the entropy itself, but in the mutual information between two variables X and Y. The mutual information "I_{XY}" measures the statistical dependence by the distance to the independent situation (Cover and Thomas, 2006; Shannon, 1948) given by

$$I_{XY} = \sum_{i,j} p(x_i, y_j) \log_2 \left(\frac{p(x_i, y_j)}{p(x_i) p(y_j)} \right) \quad \text{(eq. 4)}$$

Therefore, when X and Y are independent $p(x_i, y_j) = p(x_i) * p(y_j)$, so $I_{XY} = 0$ bits.

The mutual information can also be rewritten as the difference between the entropy of X and the conditional entropy of X given Y:

$$I_{XY} = H(X) - H(X|Y) \quad \text{(eq. 5)}$$

Where H(X) is the entropy already described (eq.1) and

$$H(X|Y) = -\sum_j p(y_j) \sum_i p(x_i|y_j) * \log_2 p(x_i|y_j) \quad \text{(eq. 6)}$$

Interestingly, if we consider a neuron stimulated repetitively by the same stimulus, we can define X as the response of the neuron to the stimulus and Y as the stimulus received by the neuron (Borst and Theunissen, 1999). In that case, H(X) can be interpreted as the total entropy (quantifying the average variability of the neuron response during one trial), also called H_S. H(X|Y) can be interpreted as the noise entropy H_N, quantifying the variability of the neuron response across the trials. In that case,

$$I_{SN} = H_S - H_N \quad \text{(eq. 7)}$$

Where Hs is the average entropy over every trials and:

$$H_N = -\langle \sum_i p(x_i)_\tau * \log_2 p(x_i)_\tau \rangle_\tau \quad \text{(eq. 8)}$$

where $p(x_i)_\tau$ is the probability of finding the configuration x_i at a time τ over all the acquired trials of an experiment (Juusola and de Polavieja, 2003; de Polavieja et al., 2005; Strong et al., 1998). Finally, we can obtain the information transfer rate R, by using the quadratic extrapolations method and dividing by the time sampling (Juusola and de Polavieja, 2003; de Polavieja et al., 2005; Strong et al., 1998), as:

$$R = R_S - R_N = \lim_{T\to\infty} \frac{1}{T} \lim_{v\to\infty} \lim_{Size\to\infty} \left(H_S^{T,v,Size} - H_N^{T,v,Size}\right) \quad \text{(eq. 3)}$$

where R_S is the entropy rate of the signal and R_N is the entropy rate of the noise (see Methods for description of the quadratic extrapolations method). In practical terms, this means to acquire multiple recordings of the same experiments, apply the quadratic extrapolations method first on each trial and average the results to obtain R_S. Then, to apply the same method across the trials for every time τ and average the results to obtain R_N. The information transfer rate R is thus the rate of the mutual information transferred between the stimulation protocol and the acquired trials.

In order to apply this method to electrophysiological signals, we used the same model as in the paragraph 3.2. In a first step, the synapses number was chosen to obtain a spiking frequency of 1 Hz. We ran 20 trials of 5 seconds with the same train of synapses (Figure 4A, left). In order to introduce some randomness in the spiking between trials, a small Gaussian noise current was also injected (Figure 4A, left). We calculated R_S and R_N using the quadratic extrapolations method. (Figure 4A, middle) and subtracted R_N to R_S to obtain the information transfer rate (here presented in bits/s) (Figure 4A, right). We then reproduced this protocol with various numbers of synapses to obtain different spiking frequencies. As expected, when we increased the number of synapses, we increased the spiking frequency and the information transfer rate between our stimulation and the response (Figure 4A, right). This measure follows a linear trend, really similar to previous results obtained in literature (Juusola and de Polavieja, 2003; de Polavieja et al., 2005).

As already described (Figure 1D, right), the PNG format is line-wise. The compression algorithm will thus be sensitive to the orientation of the image we have to compress. To estimate the PNG Rate of the signal, we converted our voltage signals to an 8-bits PNG image (256 levels of grey). As our signals are 20 trials of 5s at 10 kHz sampling, this yielded a 1 000 000 pixels of 256 grey scale image (Figure 4B, left). We saved this first version of the image, measured the size of the files on the hard drive, divided this number by the number of pixels in the image and multiplied the value by the sampling (10 kHz) to obtain the PNG Rate of the signal in Bytes/s. To estimate the PNG Rate of the noise, we simply rotated the image 90 degrees and saved it again to PNG format. This constrains the algorithm to calculate the entropy through the acquired trials and not through the signal itself, thus estimating the entropy of the noise through every trials (Figure 4B, middle). We measured the size of the newly generated file, divided again by the number of pixels in the image and multiplied the value by the sampling (10 kHz) to obtain the PNG Rate of the noise in Bytes/s. Finally, we subtracted the PNG Rate of the noise to the PNG Rate of the signal. As we can see, this difference of PNG Rates follows a linear behavior, increasing with AP frequency similarly to the direct measure of the information transfer rate (Figure 4B, right). We concluded that the PNG method allows accurate estimation of information transfer rate modifications through different conditions in electrophysiological data (here different spiking frequencies).

3.4 Synaptic information efficacy estimation

As a second example, we reproduced the protocol made by (London et al., 2002) to estimate the information transfer between one synapse and the postsynaptic neuron spiking (also called Synaptic Information Efficacy, SIE). In this study, the authors showed that a larger synapse drived the postsynaptic spiking in a greater manner, which increase the SIE. To reproduce this result, we used the model described in the previous paragraphs. We stimulated the model during 5 seconds with 750 synapses to get a spiking frequency around 5Hz. Moreover, we added a supplementary synapse stimulating the model regularly every 200 ms. When the EPSP size of this supplementary synapse (wSyn_supp) was weak, this synapse did not drive the spiking of the model (Figure 4C, up left). However, when wSyn_supp was strong, this synapse drove the spiking of the model (Figure 4C, down left). We made 100 trials for each wSyn_supp and at each trial the onset time and amplitude of the others synapses were chosen randomly. We down-sampled our signal to 3 kHz and binarized it to 0 and 1, depending on the presence of APs or not similarly to (London et al., 2002). After calculating the information rate transfer using the quadratic extrapolations method, we obtained a sigmoid curve similar to previously published results (London et al., 2002) (Figure 4C, middle). To calculate the PNG Rate on binarized signals, we first converted our voltage signals to a 1-bit PNG image (2 levels of grey). As our signals are 100 trials of 5s at 3 kHz sampling, this yielded an image of 15 000 * 100 (= 1 500 000) pixels of 2 possible values. Similarly to what has been described in paragraph 3.3, to obtain the PNG Rate of the signal, we measured the size of the file, divided it by the number of pixels and multiplied it by the sampling to obtain a value in Bytes/s. To obtain the PNG entropy rate of the noise, we rotated the image 90 degrees, measured the size of this new file, divided it by the number of pixels and multiplied it by the sampling to obtain a value in Bytes/s. As expected, the difference between the PNG Rate of the signal and the PNG Rate of the noise followed a sigmoid curve really similar to the one calculated by the quadratic extrapolations method (Figure 4C, right).

From this, we concluded that by saving multiple trials of the same experiment as a single PNG file, we can estimate the PNG Rate of the signal. And by simply rotating this same file 90 degrees and saving it again, we can estimate the PNG Rate of the noise. The difference between those two values follows the same behavior than measuring the information transfer rate between the stimulation protocol and the multiple recorded responses. Therefore, PNG Rate method is suitable to compare the Synaptic Information Efficacy of different sizes synapses.

3.5 Application to Place Fields

Some hippocampal cells have their firing rate modulated by the animal position, discharging specifically at a spatial region known as the place field of the cell (O'Keefe and Dostrovsky, 1971). Properly identifying these cells requires estimates of the information contained in spikes about navigational features (i.e., position, speed, head angle). The main metrics used to estimate

this type of information were proposed by (Skaggs et al., 1993) and are derivations from Shannon's mutual information. By definition, the experiment conditions are less controlled than in our previous simulations, as the experimenter cannot be certain that the animal will explore its full environment.

We generated a set of data mimicking an animal running randomly in an enclosed environment (Figure 5A). This closed environment was divided in 20*20 bins of space; the mock animal was put at a random point in the environment and was let to stay in for different durations. Animal speed and occupancy were considered constant over time and of 1 second per bin. We defined a simple "random walk" algorithm where at each time, the next position of the animal was chosen randomly between the 8 adjacent space bins and its own bin. This gives a random pathway exploring only some part of the environment, passing through the same space bin multiple times, etc... At each step, white noise of 1 spike was emitted with a chance of 0.1. In addition we set a mock place field, where until 20 spikes could be emitted following a Gaussian centered in the middle of the environment (SD = 3 bins). This place field had an increasing chance to fire (from 0 to 1), in order to mimic place fields of increasing strengths. This gave a crude but versatile place field simulation, where we could not control the path of the mock animal (Figure 5A).

To estimate the spatial information contained in the firing rate of each cell, we computed the I_{sec} metric as described in (Skaggs et al., 1993; Souza et al., 2018), as it is equivalent to the Mutual Information from the average firing rate (over trials) in the N space bins using the following definition:

$$MI \approx I_{SEC} = \sum_{i=1}^{N} p_i \lambda_i \log_2 \frac{\lambda_i}{\lambda} \qquad \text{(eq. 9)}$$

Where λ_i is the mean firing rate in the i-th space bin and p_i the occupancy ratio of the bin, while λ is the overall mean firing rate of the cell. I_{sec} measures information rate in bits per second (Skaggs et al., 1993). This way of computing MI looks extremely simple, but by using it the user has to keep in mind that he makes four essential assumptions: **i**) The information is purely encoded by the spike frequency; **ii**) The position of the animal is the only parameter which could influence the spike frequency; **iii**) The binning in time and space is ideal and **iv**) The spiking frequency of the noise and the place field will be similar between animals (But see (Souza et al., 2018) for an attempt to correct for this bias). By doing so, we can simplify our entropy and MI calculations to a single probability space and obtain this equation. The direct methods and the source compression methods such as the PNG Rate we present here are generic ways of calculating entropy, without making any assumptions. However, in these simulated data we know that the position will be the only parameter affecting the spiking frequency, and thus the PNG Rate method should give equivalent results to equation 9.

We ran 10 simulations of 10 000 steps for each value of place field strength and calculated the MI according to (eq. 9). We obtained an increase of the MI with the strength of the place field

(Figure 5C, left), as expected. To use our PNG algorithm, we simply traversed all the space bins with a pairing function, accumulating the spike values if there was one (Figure 5B). This gave us a 2D image with a 20*20 = 440 maximum width and a height depending on the number of times the mock animal went on the same position (Figure 5B, right). There were "holes" as it never went through every position the same amount of time, but we considered them as empty with 0 spike. We saved those images in both orientations, calculated the PNG rate and subtracted one to the other. The obtained curve has similar characteristics to the previously calculated MI (Figure 5C, right).

From this third test, we conclude that we can apply the same algorithm to more complex data like Place Fields recordings. Even if the data are not homogenous, a simple pairing transform can map all 2D coordinates to unique 1D index, progressively building a 2D image (Figure 5B). This image can then be saved as PNG to estimate its Entropy Rate and Mutual Information.

3.4 Application to histology

Another way to understand entropy is that it is a representation of complexity of a signal (Cover and Thomas, 2006). For example, (Wagstaff and Corsetti, 2010) used the PNG compression algorithm to evaluate the complexity of biogenic and abiogenic stromatolites. As a quick example, we took one of the famous drawings of a cortical column by Santiago Ramon y Cajal (Cajal, 1899) (Figure 6A, top, Wikimedia Commons). We saved each 1-pixel column of this picture as an 8-bits PNG file and measured its size on the hard drive. As we see, the size of the columns as PNG files changes with the different layers of the cortical stack, illustrating the differences in cell density and dendrites arborizations (Figure 6A, bottom). It allows a quantitative description of the layers' complexity.

In the same spirit, we used the ddAC Neuron example from the FIJI distribution of the ImageJ software (Schindelin et al., 2012). This reconstructed drosophila neuron (Figure 6Ba) is a classic example used for Sholl analysis (Ferreira et al., 2014; Sholl, 1953), (see https://imagej.net/Sholl_Analysis). This analysis estimates the complexity of an arborization by drawing concentric circles centered on the soma of the neuron and counting the number of intersections between those circles and the dendrites. The more intersections, the more complex is the dendritic tree. We realized a cylindrical anamorphosis centered on the soma of the ddAC neuron (Figure 6Bb) and saved each column of this new rectangular image as PNG files. As a result, the size of those files grew with the distance from soma, reaching the same peak than a Sholl analysis made with default settings in Fiji (Figure 6Bc). Of course, it is also possible to simply tile the original image in smaller PNG files and save them independently. The size of these files will give an idea of the complexity of the area covered by the tile (Figure 6Bd).

In a final example, we used a group of images made by Dieter Brandner and Ginger Withers available in the Cell Image Library (http://cellimagelibrary.org/groups/3006). These images are under Creative Common Attribution Licence and show the growth of neuronal cultures from 2 to

7 days In-Vitro. They show two stainings, for tubulin and MAP2. They are suitable to our needs as all the images have the same dimensions and resolution. We kept only the MAP2 channel as it reveals the dendrite morphology, converted the images to 8-bits grey scale (256 grey levels) and thresholded them to remove the background (Figure 6C, left and middle). We then saved all the images to PNG, measured the size of the files on the hard drive and divided this number by the number of visible somas, in order to make a quick normalization by the culture density. As expected, this ratio File Size / Number of Cells increases with the number of days in culture, revealing the dendrite growth (Figure 6C, right).

From this fourth test, we showed that we can use the PNG format to estimate the entropy of 2D images as well, and this can be used to estimate dendrite growth or local complexity of an image.

4 Discussion

Entropy measurement can be a tool of choice in neuroscience, as it applies to many different types of data; it can capture nonlinear interactions, and is model independent. However, an accurate measure can be difficult as it is prone to a sampling bias depending of the size of the recorded signal, its quantization levels and its sampling. There are multiple ways to compensate for it, but none of them trivial. In this paper, we showed that it is possible to estimate the entropy rate of neuroscience data simply by compressing them in PNG format, measuring the size of the file on the hard drive and dividing by the number of pixels. We called this measure the PNG Rate. The principle relies on the Source Coding Theorem specifying that one cannot compress a signal more than its entropy rate multiplied by its size. We showed first that the PNG Rate correlates linearly with the calculated Entropy Rate of signals made of Uniform white noise (Figure 1). Then, we showed that the PNG Rate needs a minimal amount of data points to converge to a stable value. This allows comparing different files of different sizes, as long as we reached this stable rate (Figure 2). Moreover, we showed that this PNG Rate method is suitable to replace methods used in previously published articles, such as the role of AP frequency in Entropy Rate ((de Polavieja et al., 2005), Figure 3 and 4) or the impact of synaptic strength on the postsynaptic firing ((London et al., 2002), Figure 4). Finally, we showed that this method is applicable to the detection of place cells or the estimation of the complexity of neuronal arborization (Figures 5 and 6).

4.1 Drawbacks of the PNG method

The main drawback of this method is that the PNG Rate is not the absolute value of the entropy rate of the signal. Even if entropy bits and computer bytes do share similar names, in no cases should we exchange one for the other. The PNG Rate is a way to estimate the evolution of entropy, considering all other parameters unchanged. As so, PNG files must be of the same dynamic range and saved with the same software. A PNG file is composed of a header, critical chunks and non-essential ancillary chunks (See Methods). Different software will save different

data in the ancillary chunks, may filter the signal before compressing it and thus will change the size of the file, independently of the compressed signal.

Other works described how to normalize the compressed chain in order to infer the original entropy value (Avinery et al., 2019). But the experimenter has to keep in mind that compression algorithms perform better with long data chains and convergence to entropy rate is slow (see (Baronchelli et al., 2005; Benedetto et al., 2002; Goodman, 2002; Khmelev and Teahan, 2003) for an extensive discussion about the benefits and drawbacks of compression algorithms). We show here that as long as we have enough pixels in the generated images, the PNG Rate will converge toward a stable value (Figure 2 and 3), which allows comparing recordings of different lengths. This PNG Rate value is not the Entropy Rate itself, but methods able to make comparisons between conditions are often required and this method fits in this situation.

4.2 Advantages of the PNG method

The main advantage of this method is that it relies on previously developed compression algorithms that were already shown as optimal (Huffman, 1952; Ziv and Lempel, 1977). Moreover, it does not need any specialized software or any knowledge in programming language, as the PNG format is ubiquitous in informatics. For example, the ImageJ software is widely used in neuroscience and can export data as PNG.

A second advantage is the speed of execution. As an example, the information transfer rates calculation (Figure 4) took a bit more than 2 hours for the quadratic extrapolations method. Saving the same signals in PNG to calculate the PNG Rates took less than 30 seconds on the same laptop computer.

As so, this method is extremely easy, quick, and does not need any knowledge in mathematics for correcting the sampling bias. It is interesting to note that an experimenter will often acquire multiple recordings of the same protocol in order to infer proper statistics. This means that most of the times no supplementary experiments are needed to calculate the entropy rate of a signal, or the information transfer rate between a stimulation protocol and its recorded result.

In conclusion, we propose the PNG method as a quick-and-easy way to estimate the entropy rate of a signal or the information transfer rate between stimulation and recorded signals. It does not give the exact value of entropy rate or information transfer rate, but it is related to these values in a linear way which allows the evaluation of their evolution in different experimental conditions.

4.3 When to use it?

As shown in this study, the PNG Rate method is simple and can be used as a back-to-the-envelope way to measure any change in entropy rate or information transfer rate through different experimental conditions. It does not give the absolute value of entropy, but often the experimenter wants a simple comparison to a control situation. This method can be virtually used

on every kind of neuroscientific data. Here, we showed examples of applications on patch-clamp data, detection of place cells by extracellular spiking recordings or histological data. Moreover, if the experimenter needs to compare multiple files of different lengths, it is possible to calculate the PNG Rate in portions of the signal with different sizes and find the minimal number of points needed for the PNG Rate to stabilize. If the number of points in all experimental conditions is above this minimal number, their PNG Rates can be compared to estimate the variation of entropy rate in the different conditions. Several works used compression algorithms to estimate absolute value of entropy. However, we do not think they apply to our simple method. The first method needs to have access to the dictionary created by the compression algorithm (Baronchelli et al., 2005). However, with the PNG algorithm we do not have access to the dictionary itself. The second method needs to first estimate the maximum entropy possible by the model (Avinery et al., 2019), which is possible as well but will need more conventional algorithm to be determined.

4.4 Developments

We see multiple ways to improve this method. First, we saved our data as 8-bits PNG files, which limits the dynamic range of the file to 256 values. However, it is possible to save PNG natively as 1, 4, 8, 16 and 24 bits range, thus greatly increasing the dynamic range of the saved signal. Second, with some programming skills it is possible to remove the header and ancillary chunks of the PNG format, thus removing the size overhead (but the file will be unreadable by standard softwares). Finally, one possible way of improving the estimation of entropy rate would be to choose a better compression algorithm. We choose the PNG format as it is widely used by common softwares and it is based on LZSS and Huffman algorithms, which have been proven optimal. However, some algorithms may give a better compression rate depending on the quality of the data. As an example, the Rice compression algorithm was originally developed for the NASA Voyager missions (Rice and Plaunt, 1971). It is suboptimal but is better suited for noisy signals of low values.

In a more general direction, it is important to note that this method works with any entropy-coding compression algorithm, as long as they are loss-less. This is the case of GZip algorithms for example, used in many compression softwares such as WinRAR, PKZIP, ARJ, etc… It is thus not limited to pictures in PNG, although this format is useful for rotating the file and estimating the mutual information easily. Moreover, we apply these algorithms to 2D images, when actually the algorithm linearizes the data and works only in linear way on one dimension. There are some attempts to generalize Shannon entropy to 2D space (Azami et al., 2019; Larkin, 2016; Sparavigna, 2019), but they are out of the scope of this paper.

5 Conflict of Interest

The authors declare that the research was conducted in the absence of any commercial or financial relationships that could be construed as a potential conflict of interest.

6 Author Contributions

Project was conceived by SR. Neuronal simulations were performed by MZ. All mock-up data and analysis scripts were written by SR, data was analyzed by SR. Writing of the manuscript was shared by MZ & SR.

7 Funding

This work was funded by the Wellcome Trust Principal Fellowship (212251/Z/18/Z), and by the ERC Proof of Principle grant (767372 – NEUROCLOUD).

8 Acknowledgements

We thank Q. Bernard, C. Leterrier, V. Marra, T. Jensen, K. Zheng, S. Martiniani, R. Beck for helpful discussions. A first version of this manuscript manuscript has been released on bioRxiv (Zbili and Rama, 2020), https://doi.org/10.1101/2020.08.04.236174.

9 References

Amigó, J.M., Szczepański, J., Wajnryb, E., and Sanchez-Vives, M.V. (2004). Estimating the Entropy Rate of Spike Trains via Lempel-Ziv Complexity. Neural Comput. *16*, 717–736.

Avinery, R., Kornreich, M., and Beck, R. (2019). Universal and accessible entropy estimation using a compression algorithm. Phys. Rev. Lett. *123*, 178102.

Azami, H., da Silva, L.E.V., Omoto, A.C.M., and Humeau-Heurtier, A. (2019). Two-dimensional dispersion entropy: An information-theoretic method for irregularity analysis of images. Signal Process. Image Commun. *75*, 178–187.

Baronchelli, A., Caglioti, E., and Loreto, V. (2005). Measuring complexity with zippers. Eur. J. Phys. *26*, S69–S77.

Benedetto, D., Caglioti, E., and Loreto, V. (2002). Language Trees and Zipping. Phys. Rev. Lett. *88*, 048702.

Bialek, W., Rieke, F., Steveninck, R. de R. van, and Warland, D. (1991). Reading a neural code. Science *252*, 1854–1857.

Bian, N., Liang, F., Fu, H., and Lei, B. (2019). A Deep Image Compression Framework for Face Recognition. ArXiv190701714 Cs.

Borst, A., and Theunissen, F.E. (1999). Information theory and neural coding. Nat. Neurosci. *2*, 947–957.

Cajal, S.R. (1899). Comparative study of the sensory areas of the human cortex.

Cover, T., and Thomas, J. (2006). Elements of Information Theory, 2nd Edition | Wiley.

Deutsch, P. (1996). DEFLATE Compressed Data Format Specification version 1.3.

Ferreira, T.A., Blackman, A.V., Oyrer, J., Jayabal, S., Chung, A.J., Watt, A.J., Sjöström, P.J., and van Meyel, D.J. (2014). Neuronal morphometry directly from bitmap images. Nat. Methods *11*, 982–984.

Goodman, J. (2002). Extended Comment on Language Trees and Zipping. ArXivcond-Mat0202383.

Hou, Y., Zheng, L., and Gould, S. (2020). Learning to Structure an Image with Few Colors. ArXiv200307848 Cs.

Hu, W., Tian, C., Li, T., Yang, M., Hou, H., and Shu, Y. (2009). Distinct contributions of Nav1.6 and Nav1.2 in action potential initiation and backpropagation. Nat. Neurosci. *12*, 996–1002.

Huffman, D.A. (1952). A Method for the Construction of Minimum-Redundancy Codes. Proc. IRE *40*, 1098–1101.

Ince, R.A.A., Giordano, B.L., Kayser, C., Rousselet, G.A., Gross, J., and Schyns, P.G. (2017). A statistical framework for neuroimaging data analysis based on mutual information estimated via a gaussian copula. Hum. Brain Mapp. *38*, 1541–1573.

Ito, S., Hansen, M.E., Heiland, R., Lumsdaine, A., Litke, A.M., and Beggs, J.M. (2011). Extending Transfer Entropy Improves Identification of Effective Connectivity in a Spiking Cortical Network Model. PLoS ONE *6*.

Juusola, M., and de Polavieja, G.G. (2003). The rate of information transfer of naturalistic stimulation by graded potentials. J. Gen. Physiol. *122*, 191–206.

Khmelev, D.V., and Teahan, W.J. (2003). On an Application of Relative Entropy. ArXivcond-Mat0205521.

Larkin, K.G. (2016). Reflections on Shannon Information: In search of a natural information-entropy for images. ArXiv160901117 Cs Math.

Larsson, N.J. (1996). Extended Application of Suffix Trees to Data Compression. In In Data Compression Conference, pp. 190–199.

Larsson, N.J. (1999). Structures of String Matching and Data Compression. thesis/docmono. Lund University.

Lefort, S., Tomm, C., Floyd Sarria, J.-C., and Petersen, C.C.H. (2009). The excitatory neuronal network of the C2 barrel column in mouse primary somatosensory cortex. Neuron *61*, 301–316.

London, M., Schreibman, A., Häusser, M., Larkum, M.E., and Segev, I. (2002). The information efficacy of a synapse. Nat. Neurosci. *5*, 332–340.

Magri, C., Whittingstall, K., Singh, V., Logothetis, N.K., and Panzeri, S. (2009). A toolbox for the fast information analysis of multiple-site LFP, EEG and spike train recordings. BMC Neurosci. *10*, 81.

Martiniani, S., Chaikin, P.M., and Levine, D. (2019). Quantifying Hidden Order out of Equilibrium. Phys. Rev. X *9*, 011031.

Martiniani, S., Lemberg, Y., Chaikin, P.M., and Levine, D. (2020). Correlation lengths in the language of computable information. ArXiv200403502 Cond-Mat Physicsnlin Physicsphysics.

Mentzer, F., Van Gool, L., and Tschannen, M. (2020). Learning Better Lossless Compression Using Lossy Compression. ArXiv200310184 Cs Eess.

Nemenman, I., Bialek, W., and de Ruyter van Steveninck, R. (2004). Entropy and information in neural spike trains: progress on the sampling problem. Phys. Rev. E Stat. Nonlin. Soft Matter Phys. *69*, 056111.

O'Keefe, J., and Dostrovsky, J. (1971). The hippocampus as a spatial map. Preliminary evidence from unit activity in the freely-moving rat. Brain Res. *34*, 171–175.

Paninski, L. (2003). Convergence properties of three spike-triggered analysis techniques. Netw. Bristol Engl. *14*, 437–464.

Panzeri, S., and Treves, A. (1996). Analytical estimates of limited sampling biases in different information measures. Netw. Bristol Engl. *7*, 87–107.

Panzeri, S., Senatore, R., Montemurro, M.A., and Petersen, R.S. (2007). Correcting for the sampling bias problem in spike train information measures. J. Neurophysiol. *98*, 1064–1072.

Piasini, E., and Panzeri, S. (2019). Information Theory in Neuroscience. Entropy *21*, 62.

de Polavieja, G.G., Harsch, A., Kleppe, I., Robinson, H.P.C., and Juusola, M. (2005). Stimulus history reliably shapes action potential waveforms of cortical neurons. J. Neurosci. Off. J. Soc. Neurosci. *25*, 5657–5665.

Rice, R., and Plaunt, J. (1971). Adaptive Variable-Length Coding for Efficient Compression of Spacecraft Television Data. IEEE Trans. Commun. Technol. *19*, 889–897.

Rueden, C.T., Schindelin, J., Hiner, M.C., DeZonia, B.E., Walter, A.E., Arena, E.T., and Eliceiri, K.W. (2017). ImageJ2: ImageJ for the next generation of scientific image data. BMC Bioinformatics *18*, 529.

Safaai, H., Onken, A., Harvey, C.D., and Panzeri, S. (2018). Information estimation using nonparametric copulas. Phys. Rev. E *98*.

Schindelin, J., Arganda-Carreras, I., Frise, E., Kaynig, V., Longair, M., Pietzsch, T., Preibisch, S., Rueden, C., Saalfeld, S., Schmid, B., et al. (2012). Fiji: an open-source platform for biological-image analysis. Nat. Methods *9*, 676–682.

Shannon, C.E. (1948). A Mathematical Theory of Communication. Bell Syst. Tech. J. *27*, 379–423.

Sholl, D.A. (1953). Dendritic organization in the neurons of the visual and motor cortices of the cat. J. Anat. *87*, 387–406.

Skaggs, W.E., McNaughton, B.L., Gothard, K.M., and Markus, E.J. (1993). An Information-Theoretic Approach to Deciphering the Hippocampal Code. In In, (Morgan Kaufmann), pp. 1030–1037.

Souza, B.C., Pavão, R., Belchior, H., and Tort, A.B.L. (2018). On Information Metrics for Spatial Coding. Neuroscience *375*, 62–73.

Sparavigna, A.C. (2019). Entropy in Image Analysis.

Storer, J.A., and Szymanski, T.G. (1982). Data compression via textual substitution. J. ACM *29*, 928–951.

Street, S. (2020). Upper Limit on the Thermodynamic Information Content of an Action Potential. Front. Comput. Neurosci. *14*, 37.

Strong, S.P., Koberle, R., de Ruyter van Steveninck, R.R., and Bialek, W. (1998). Entropy and Information in Neural Spike Trains. Phys. Rev. Lett. *80*, 197–200.

Timme, N.M., and Lapish, C. (2018). A Tutorial for Information Theory in Neuroscience. ENeuro *5*.

Vicente, R., Wibral, M., Lindner, M., and Pipa, G. (2011). Transfer entropy—a model-free measure of effective connectivity for the neurosciences. J. Comput. Neurosci. *30*, 45–67.

Wagstaff, K.L., and Corsetti, F.A. (2010). An evaluation of information-theoretic methods for detecting structural microbial biosignatures. Astrobiology *10*, 363–379.

Wiegand, T. (2010). Source Coding: Part I of Fundamentals of Source and Video Coding. Found. Trends® Signal Process. *4*, 1–222.

Zbili, M., and Rama, S. (2020). A quick and easy way to estimate entropy and mutual information for neuroscience. BioRxiv 2020.08.04.236174.

Ziv, J., and Lempel, A. (1977). A universal algorithm for sequential data compression. IEEE Trans. Inf. Theory *23*, 337–343.

10 Data Availability Statement

All scripts used to analyze data are available at https://github.com/Sylvain-Deposit/PNG-Entropy

The Cell Image Library group used in Figure 4 was originally obtained by Dieter Brandner and Ginger Withers and is available at http://cellimagelibrary.org/groups/3006

781

Figure Legends

1 Figure 1: comparison of entropy and PNG file size on a model case.

A) Examples of 10 000 data points of uniform white noise with growing number of grey levels and growing entropy (here showed as square picture signals). Left: 2 possible grey values, or entropy of 1. Middle: 16 possible grey values, or entropy of 4. Right: 256 possible grey values, or entropy of 8.

B) Direct calculation and quadratic extrapolations to 0 to calculate the entropy rate of the left signal in A). Left: Plotting all the entropy values to 1/Size and extrapolating to 0 to get the value for infinite size (white arrowhead). For clarity, only the condition for v = 2 is shown. Middle: plotting the obtained values at left to 1/v and extrapolating to 0 to get the value for infinite number of quantization levels (white arrowhead). Right: plotting the final values to 1/T and extrapolating to 0 to get the value for infinite number of combinations bins (black arrowhead). Note that this value is really close to 1, as expected when using a signal made of uniform white noise with 2 possible values.

C) Direct calculation and quadratic extrapolations to 0 to calculate the entropy rate of the right signal in A). Left: Only the condition for v = 2 is shown. Note that in the final graph (right), points do not follow a linear trend. When using the last 2 points for extrapolation to 0, the value is far from the expected value of 8 (red arrowhead).

D) Left: when plotted against the known entropy value, the direct method with quadratic extrapolation shows examples of sampling disaster for high values of entropy (red arrowheads). Right: when simply saving all the signals described in A) and dividing their size by the number of pixels in the image, the PNG Rate in Bytes per pixel shows a linear relationship with the Entropy Rate ($y = 0.12\,x + 0.06$, $R^2 = 0.99$). Not that this is true for pictures made either of square signals (squares plot) or linearized signals (crosses plot).

2 Figure 2: Effect of signal size on direct entropy calculation and PNG Rate.

A) Left: Example of 100 and 10 000 data points of 0 (or black) with growing amount of 1 (or white), here showed as square picture signals (10% white and 50% white, respectively). Middle: When using the direct method with quadratic extrapolation, we obtain the ideal bell-shaped curve (compare dark grey line to black dashed line). However, if our signal is short (100 points for example, light grey curve), it is impossible to calculate high entropy values. Right: normalized PNG file sizes of the same signals, showing that when we increase the number of points in the signal, we progressively fit the obtained curve toward the ideal entropy curve. This convergence seems slower than when using the direct method.

B) Left: effect of the number of points on the maximal entropy calculation via the direct method and quadratic extrapolation. For signal with few points, the curve shows a biphasic behavior revealing the sampling disaster: a signal of few points cannot be used to calculate high entropy

values. When increasing the number of points, the curve becomes accurate for every value. Right: same demonstration when using the PNG Rates. Even with few points, the curve shows a linear behavior. However, increasing the number of points modifies the slope and intercept of the linear curve, until it stabilizes to an optimal solution.

C) Left: If we plot the entropy rate versus the number of points in the signal, we see that the direct method converges quickly to the optimal value (White arrowhead on white circles, around 500 points, value of R = 0.9923 bits per point). If we plot the PNG Rate as the PNG file size divided by the number of pixels in the image versus the number of pixels in the image, we obtain a curve decreasing slowly to a stable value (Black arrow on black squares, around 10 000 points, value of P = 0.17 Bytes per pixels). Right: Same calculations made with a signal of entropy H = 2 (4 different values possible). The direct method converges in around 1000 points (R = 1.9794 bits per points) while the PNG Rate converges in around 10 000 pixels (P = 0.32 bytes per pixels).

Figure 3: PNG Rate on a model of neuronal activity.

A) Left: example of traces obtained with our model, increasing the number of synapses to obtain spiking activity from 1 Hz (top) to 20 Hz (bottom). Right: The PNG Rate (B/pixels) is linear to Entropy Rate (b/points), following $y = 0.36x - 0.02$ ($R^2 = 0.99$).

B) Impact of the simulation duration on the Entropy Rate (left) and PNG Rate (right). Entropy Rate converges toward a stable solution in around 5 seconds of recordings, or 1 sweep. The PNG Rate needs around 40 seconds to obtain a stable value. As the PNG algorithm starts by linearizing the data, this is equivalent to 8 sweeps of 5 seconds each.

Figure 4: Comparison of Mutual Information and PNG Rate on a neuronal model.

A) Left: example of 20 generated trials with the same synaptic activity. Due to the injection of a small Gaussian noise current, we obtain variability in the spiking of the different trials. Arrows show the direction used with the quadratic extrapolation method to calculate the signal entropy (R_S) and noise entropy (R_N). Middle: calculation of the Entropy Rate of the Signal (Rs) and the noise (Rn) for the full voltage of the cell for each condition. The Information transfer Rate R is the difference between Rs and Rn. Right: Information transfer Rate between the synaptic stimulation and the neuronal activity, versus the spiking frequency. This follows a linear trend ($y = 25.935\,x + 188.15$, $R^2 = 0.97$).

B) Left: Conversion of the modeled trials in A) as a 256 grey values PNG file. As the PNG conversion algorithm is line-wise, we have to save the image a first time, then rotate it 90 degrees and save it a second time (Middle). Arrows show the direction of compression. Right: the subtraction of the 2 images sizes follows a linear trend with the spiking frequency ($y = 25.55\,x - 41.2$, $R^2 = 0.98$).

C) Left: examples of rastergrams showing the impact of the supplementary synapse on our neuronal model. With a low synaptic strength (wSyn_supp = 2 mV, top), this synapse barely drives the model. With a high synaptic strength (wSyn_supp = 6 mV, bottom), the neuron spiking starts to synchronize with the occurrence of the synapse. Middle: Information transfer Rate between the activity of the supplementary synapse and the neuronal spiking. As expected, it follows a sigmoidal behavior. Right: rastergrams were saved as PNG files, rotated 90 degrees and saved again. The difference of the 2 files sizes follows a similar curve than the Information transfer Rate.

Figure 5: Application to Mutual Information from Place Fields.

A) Examples of simulated data: a mock animal with a random walk in an enclosed environment. The firing rate of each space bin was modeled as a Gaussian centered in the field, with growing probability of firing. Left: example of a 1000-steps random walk with a place field of low probability of firing (p = 0.3). Middle: example of a 10 000-steps random walk with a place field of high probability of firing (p = 1).

B) Simple explanation of the pairing function used to transform the Place field information to a 2D array to be saved in PNG format. Left: the area is divided in space bins, and each bin is given a unique index, which will be the index of the column of the future image. Middle: if we follow the patch showed with the arrow, we traverse the indexes 1, 2, 3, 6, 5, 4, 1, 2, 3, 2, 1. For each traversed index, we place a pixel with the color corresponding to the firing frequency at the corresponding column index. If we go to the same position multiple times, we simply add multiple rows to the 2D array. There will be “holes” (grey squares) as the path did not go to every position the same number of times, but we can fill them with 0 (blue squares). Right: result of this pairing function on the 20*20 arena for the example seen in A), left (top) and A), right (bottom). Right: Same data presented in A) (Left example is Top, Right example is Bottom, respectively) after pairing transform. These files were saved as PNG, rotated, saved again to obtain the difference in PNG Rates.

C) Left: Mutual Information as I_{sec} (eq. 9) versus Place Field strength, showing a clear increase when the place field has a high chance to fire. Right: Difference in PNG Rates versus Place Field strength. Both curves are similar.

Figure 6: Application to 2D data.

A) Top: original drawing of a cortical column by Santiago Ramon y Cajal. Arrow: each column of pixel was saved as a PNG file. Bottom: File size of each column as PNG, revealing the change in organization and complexity of the different layers.

B) a: ddAC Neuron from Fiji examples. b: The same neuron after a circular anamorphosis centered on the soma. Note how the complexity of the dendritic arbor changes versus distance from soma. Arrow: each column of pixel was saved as a single PNG file. c: file size of these

columns as PNG, showing the growth in complexity of the dendritic arborization (black line). As a comparison, we performed a Sholl analysis of the same image with default FIJI parameters (grey line). d: the original image was tiled in 10 squares, and each square saved as a PNG file. The sizes of these files reveal the heterogeneity of the dendritic arborization.

C) Left and Middle: examples of MAP2 stainings of Brandner and Withers neuronal cultures at 2 and 7 Days In Vitro. Note the growth in dendritic arborization through time. Right: Each image was saved into a PNG file, and the file size divided by the number of visible somas. This gives us a file size normalized by the density of the culture. This value increases with the number of Days In-Vitro, revealing the dendrite growth.

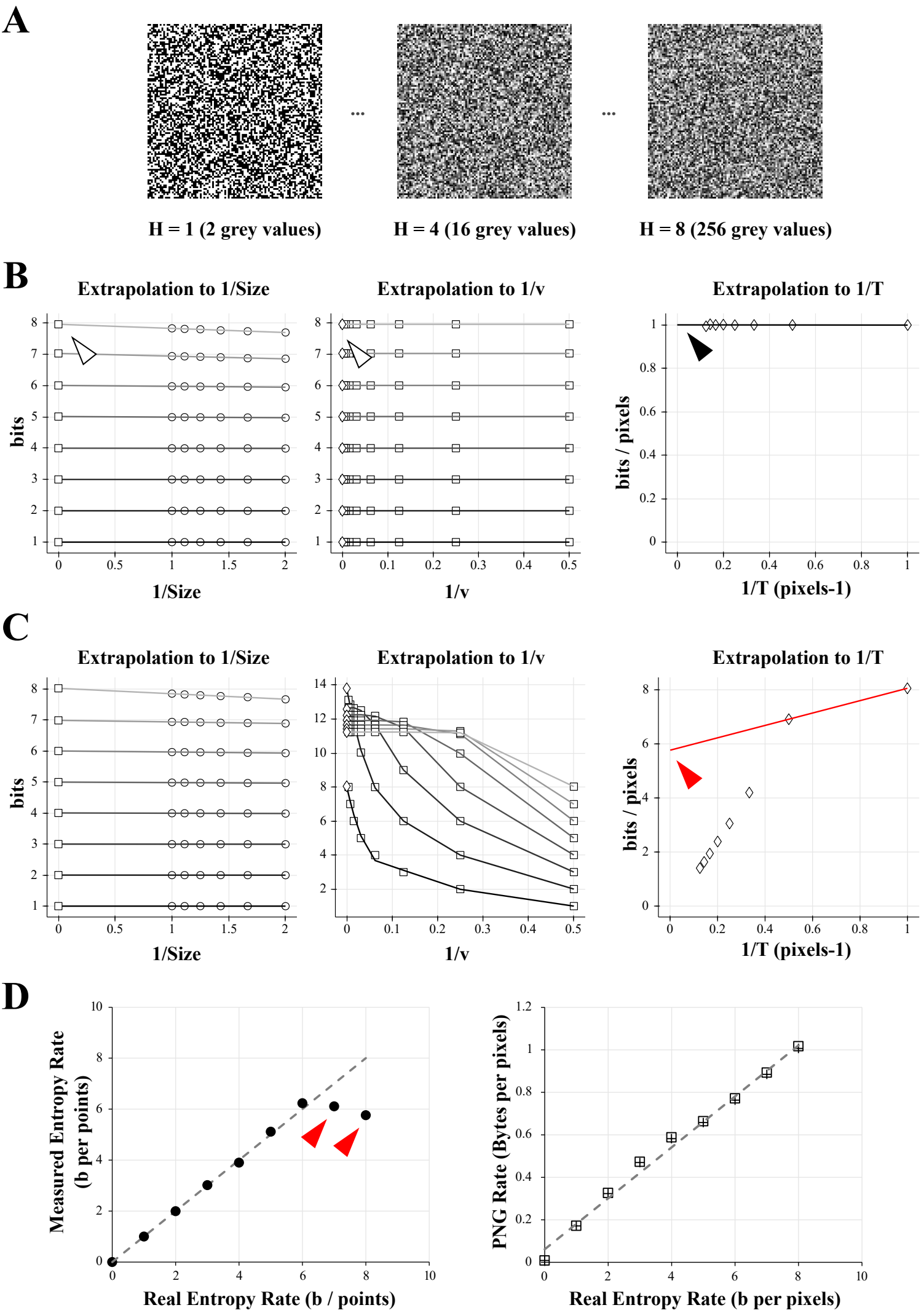
A
H = 1 (2 grey values)
H = 4 (16 grey values)
H = 8 (256 grey values)
B
Extrapolation to 1/Size
Extrapolation to 1/v
Extrapolation to 1/T
bits
1/Size
1/v
bits / pixels
1/T (pixels-1)
C
Extrapolation to 1/Size
Extrapolation to 1/v
Extrapolation to 1/T
bits
1/Size
1/v
bits / pixels
1/T (pixels-1)
D
Measured Entropy Rate (b per points)
Real Entropy Rate (b / points)
PNG Rate (Bytes per pixels)
Real Entropy Rate (b per pixels)

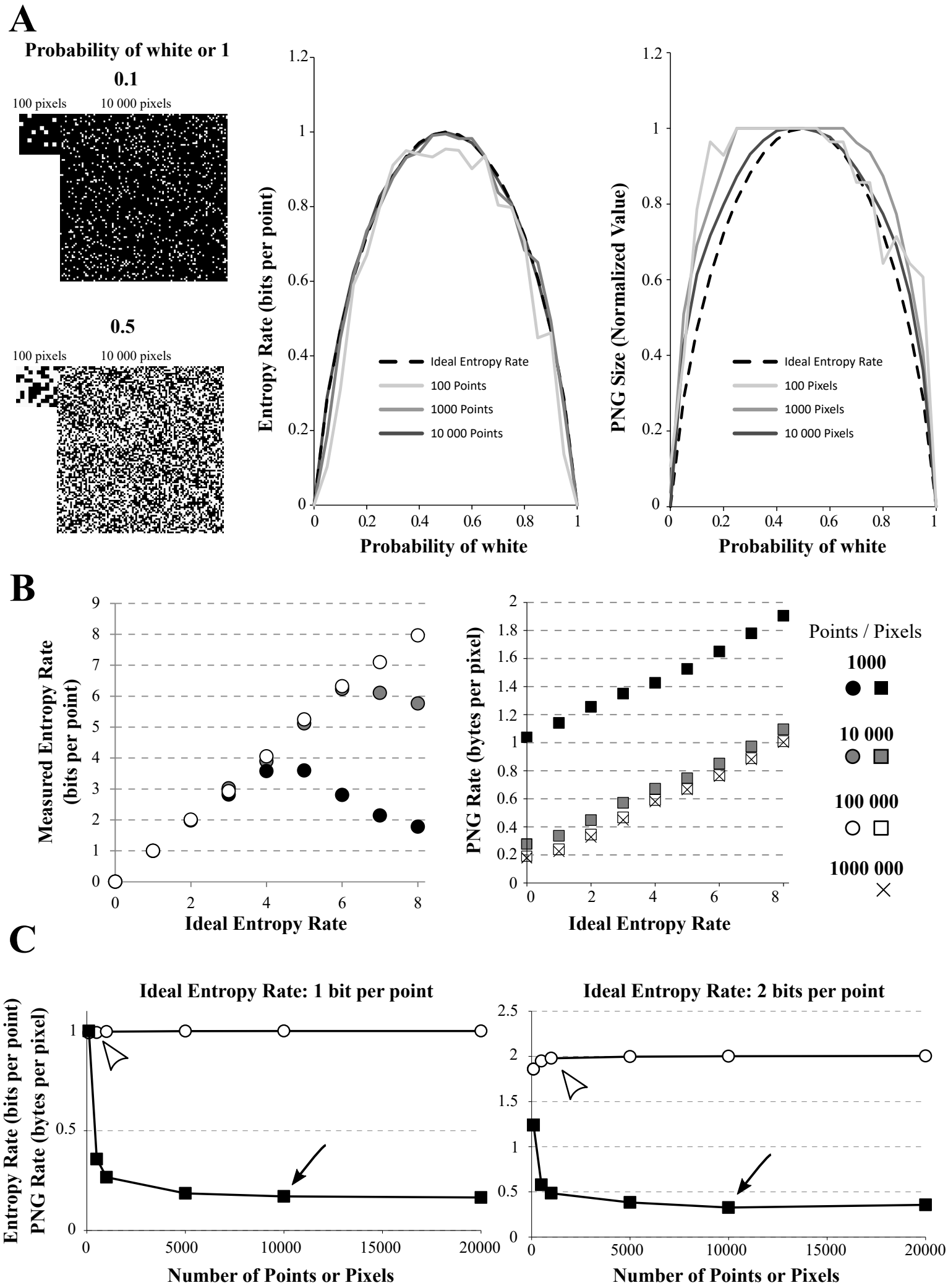
A
Probability of white or 1
0.1
100 pixels
10 000 pixels
0.5
100 pixels
10 000 pixels
Entropy Rate (bits per point)
Probability of white
Ideal Entropy Rate
100 Points
1000 Points
10 000 Points
PNG Size (Normalized Value)
Probability of white
Ideal Entropy Rate
100 Pixels
1000 Pixels
10 000 Pixels
B
Measured Entropy Rate (bits per point)
Ideal Entropy Rate
PNG Rate (bytes per pixel)
Ideal Entropy Rate
Points / Pixels
1000
10 000
100 000
1000 000
C
Ideal Entropy Rate: 1 bit per point
Entropy Rate (bits per point)
PNG Rate (bytes per pixel)
Number of Points or Pixels
Ideal Entropy Rate: 2 bits per point
Number of Points or Pixels

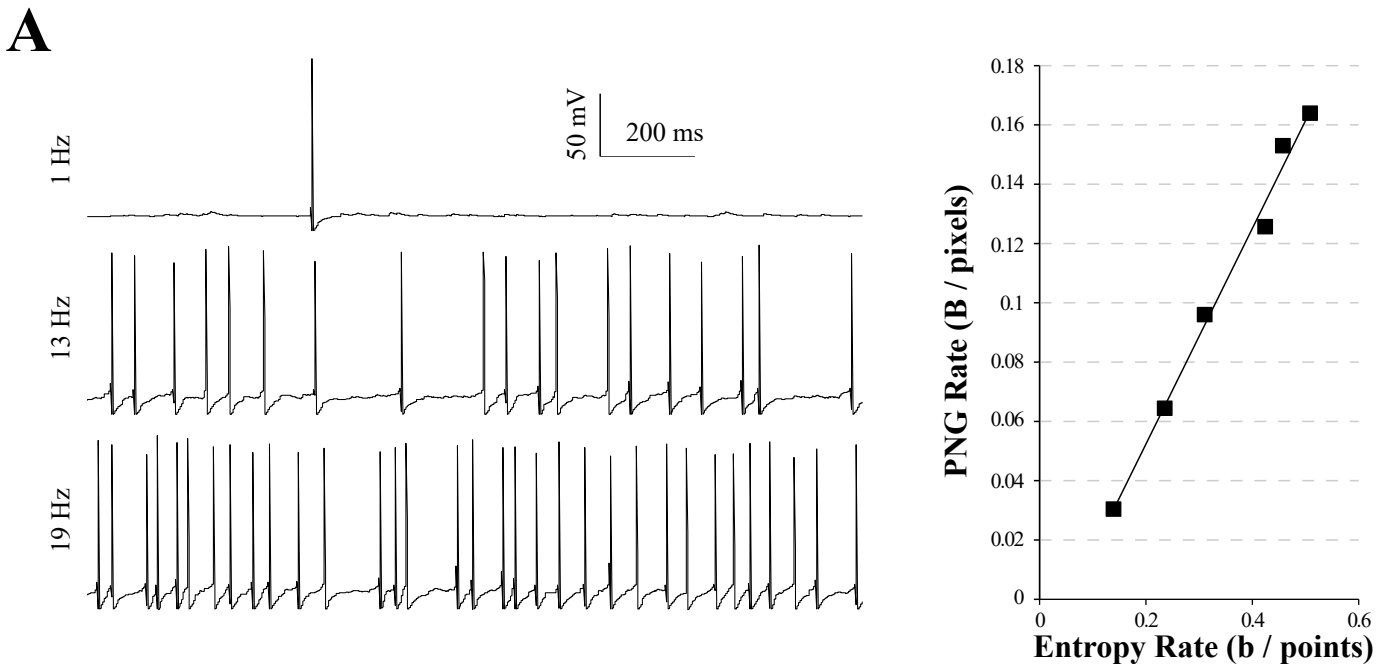
A
1 Hz
13 Hz
19 Hz
50 mV
200 ms
PNG Rate (B / pixels)
Entropy Rate (b / points)
0
0.02
0.04
0.06
0.08
0.1
0.12
0.14
0.16
0.18
0.2
0.4
0.6

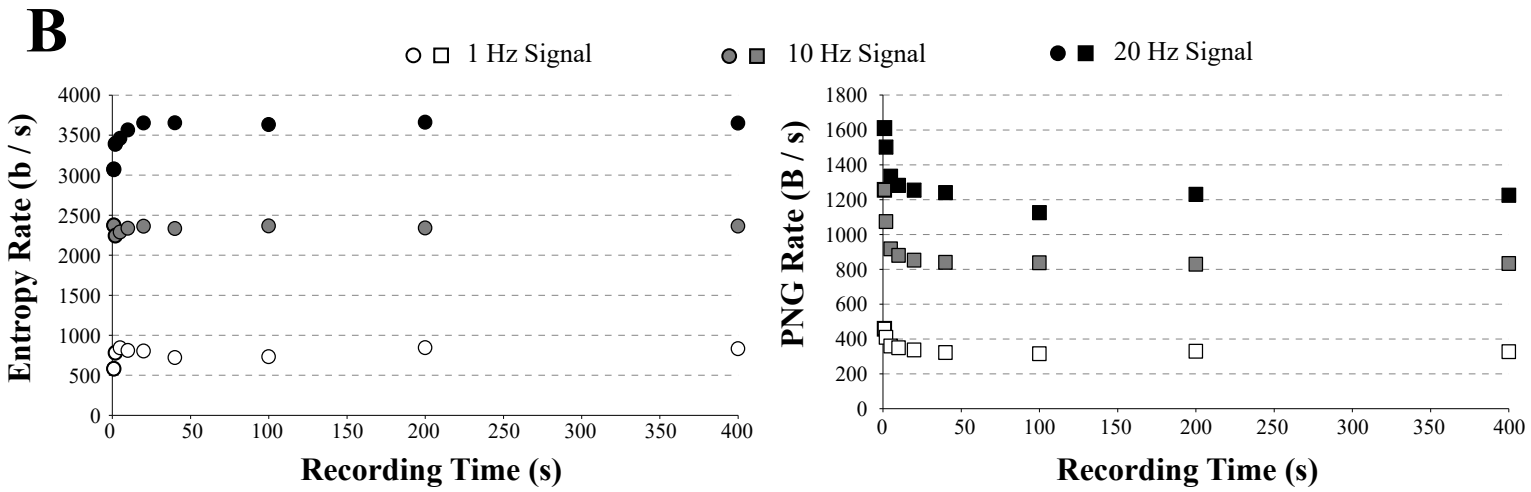
B
1 Hz Signal
10 Hz Signal
20 Hz Signal
Entropy Rate (b / s)
PNG Rate (B / s)
Recording Time (s)
Recording Time (s)
0
500
1000
1500
2000
2500
3000
3500
4000
200
400
600
800
1000
1200
1400
1600
1800
50
100
150
200
250
300
350
400

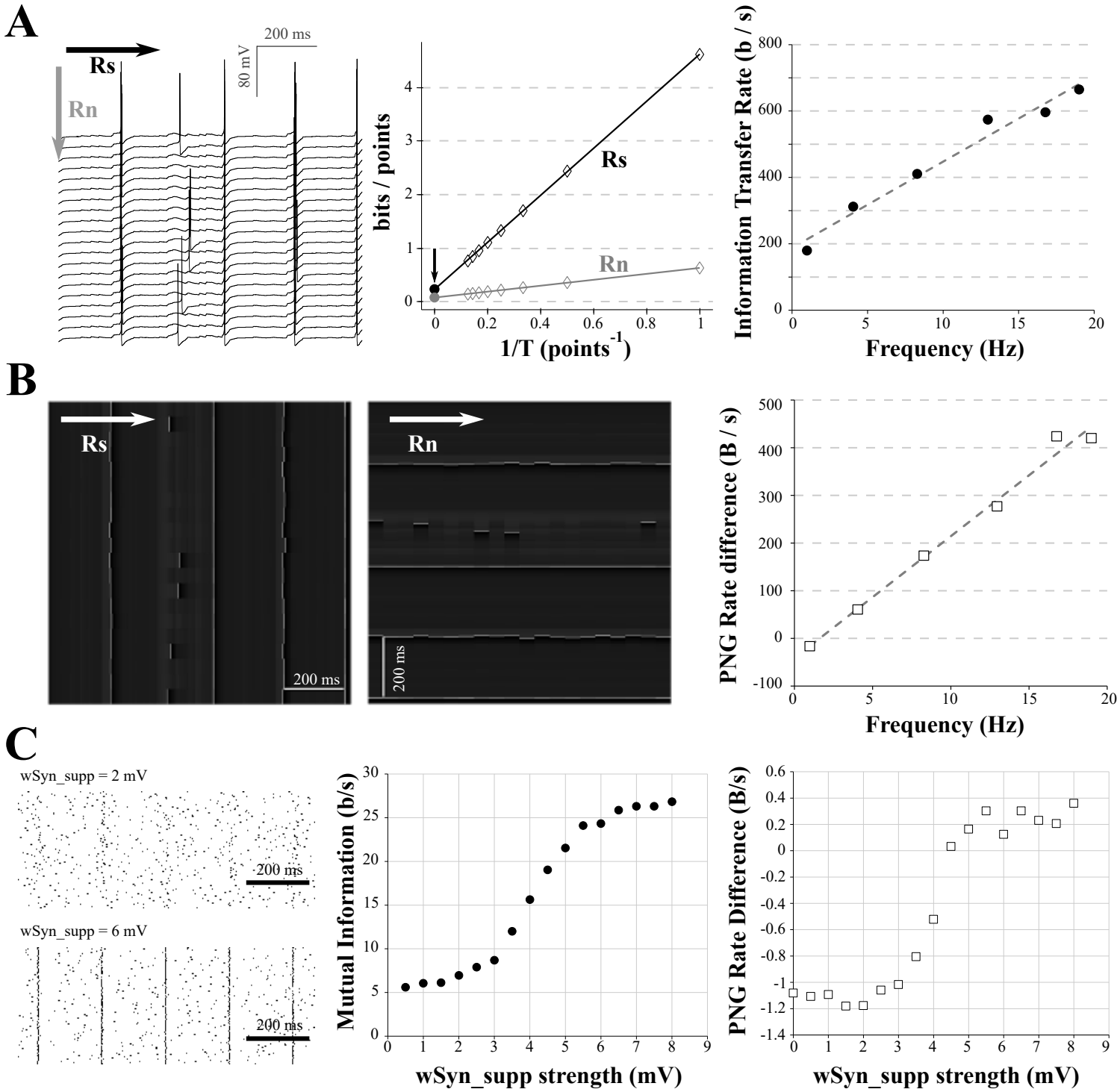
A
Rs
Rn
200 ms
80 mV
bits / points
1/T (points^{-1})
Rs
Rn
Information Transfer Rate (b / s)
Frequency (Hz)
B
Rs
Rn
200 ms
200 ms
PNG Rate difference (B / s)
Frequency (Hz)
C
wSyn_supp = 2 mV
200 ms
wSyn_supp = 6 mV
200 ms
Mutual Information (b/s)
wSyn_supp strength (mV)
PNG Rate Difference (B/s)
wSyn_supp strength (mV)

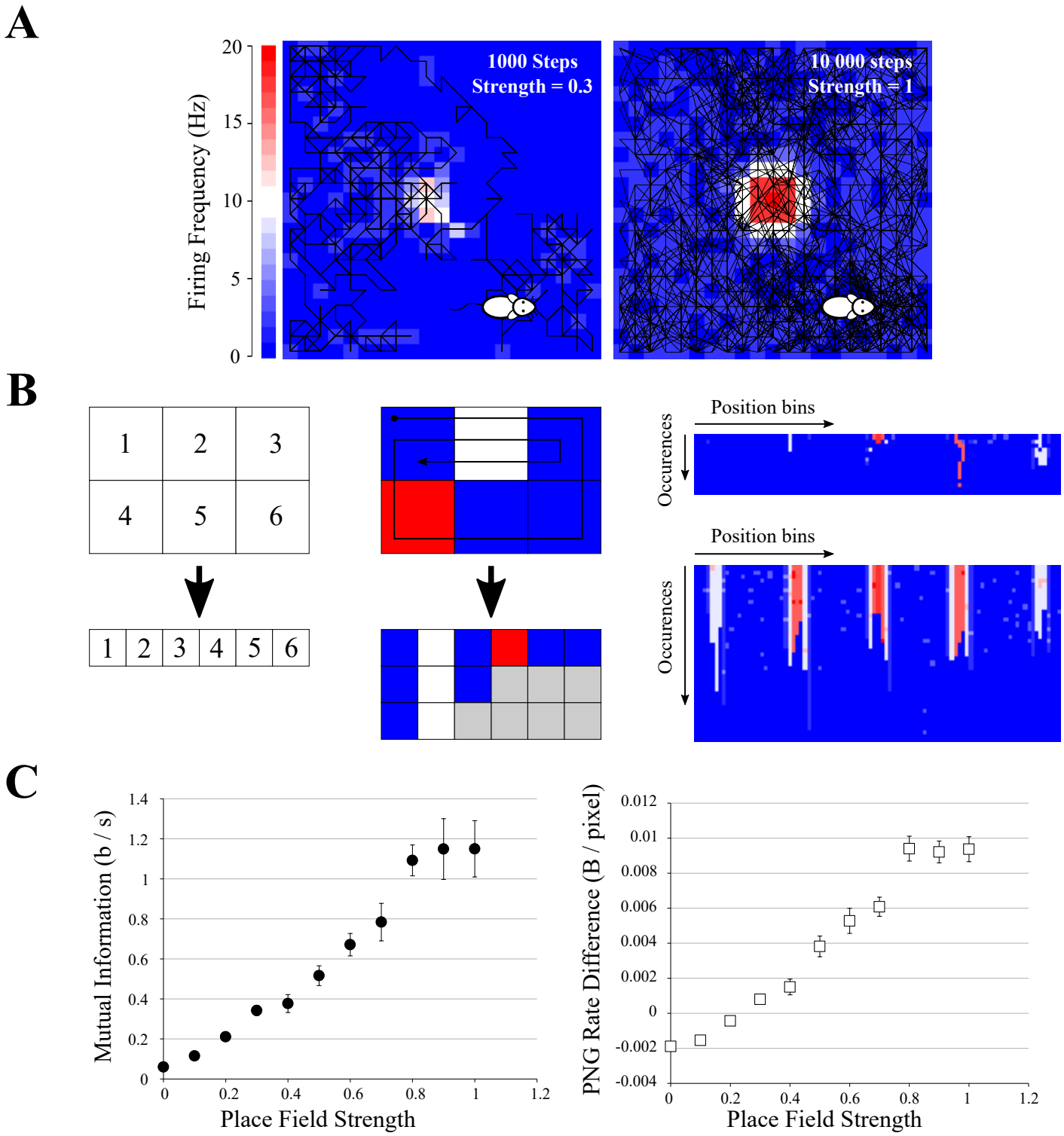
A
Firing Frequency (Hz)
20
15
10
5
0
1000 Steps
Strength = 0.3
10 000 steps
Strength = 1
B
1
2
3
4
5
6
1
2
3
4
5
6
Position bins
Occurences
Position bins
Occurences
C
Mutual Information (b / s)
1.4
1.2
1
0.8
0.6
0.4
0.2
0
0
0.2
0.4
0.6
0.8
1
1.2
Place Field Strength
PNG Rate Difference (B / pixel)
0.012
0.01
0.008
0.006
0.004
0.002
0
-0.002
-0.004
0
0.2
0.4
0.6
0.8
1
1.2
Place Field Strength

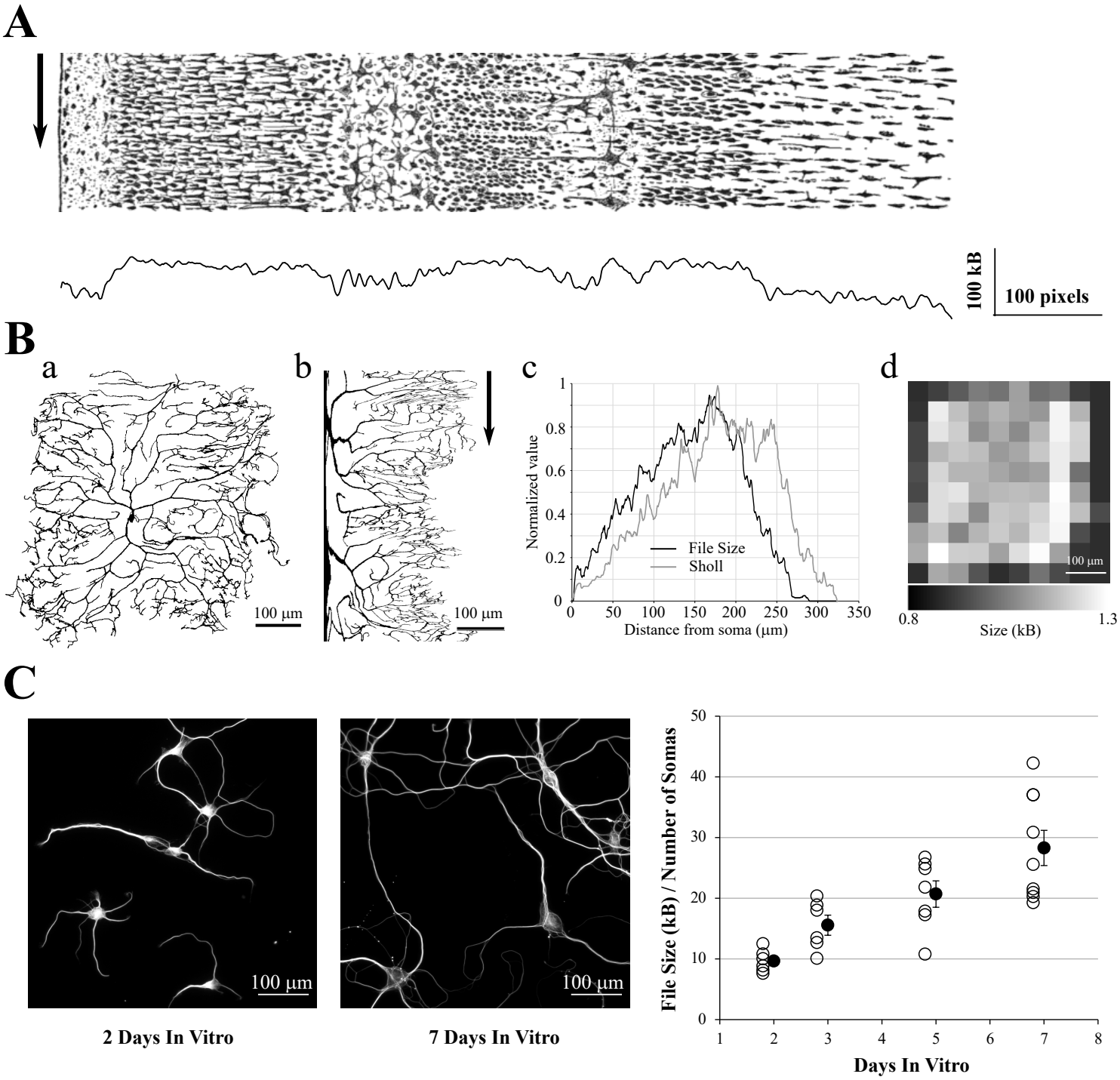
A
100 kB
100 pixels
B
a
100 µm
b
100 µm
c
Normalized value
File Size
Sholl
Distance from soma (µm)
d
100 µm
0.8
1.3
Size (kB)
C
100 µm
2 Days In Vitro
100 µm
7 Days In Vitro
File Size (kB) / Number of Somas
Days In Vitro